

A Robust Human-robot Collaborative Control Approach Based on Model Predictive Control

Tianyi Zeng, Abdelkhalick Mohammad, Andres Gamos Madrigal, Dragos Axinte and Max Keedwell

Abstract—Human skill based robotic control to perform critical manufacturing operations (e.g. repair and inspection for high-value assets) can reduce scrap rates and increase overall profitability in the industrial community. In this study, a human-robotic collaborative control system is developed for accurate path tracking subject to unknown external disturbances and multiple physical constraints. This is achieved by designing a model predictive control with a sliding mode disturbance rejection term. To rule out the possibility of the constraints violation caused by external disturbances, tightened constraints are formulated to generate the control input signal. The proposed controller drives the robotic system remotely with enhanced smoothness and real-time human modification on the outputted performance so that the human experience can be fully transferred to robotic systems. The efficacy of the proposed collaborative control system is verified by both Monte-Carlo simulation with 200 cases and experimental results including Tungsten Inert Gas (TIG) welding based on a Universal Robot (UR) 5e with 6 Degree-of-Freedom.

Index Terms—Remote control, Universal Robot, Model predictive control; Disturbance rejection

I. INTRODUCTION

INDUSTRIAL robots are widely used in manufacturing and assembly lines, such as the automotive and white-goods industries as they offer major improvements in productivity, safety, ease of programming, portability and cost saving [1], [2]. Much effort has been put into the design of robotic solutions, e.g. 6 degree-of-freedom (DoF) with payload capacities improvements to assist a wide range of applications and industries [3]. Nevertheless, their controllers still seem to work based on point-to-point vectoring of the desired paths as this is acceptable for many applications, such as spot welding, assembly, part manipulations and even machining where such operations are often used in the automotive industry. However, the stability of moving robotic end-effectors is very sensitive when it comes to continuous operations with high accuracy requirements such as welding/gluing for curved paths where a small change in both the distance and the velocity between the end effector and the component may produce a considerable variation in the process outcomes [4], [5]. Taking further the example of robotic welding/gluing as processes requiring "smooth" and continuum end-effector manipulations, the robot should keep moving after each waypoint without any stop during the whole process. Due to the shortage of the skilled worker, especially the experienced welder (e.g. left-handed welder), it would be desirable that industrial robots can provide continuous velocity to guarantee this smoothness so that it

can mimic or replicate the characteristics which human limbs possess.

Therefore, concern over control performance with the smoothness not only in the path but also in velocity to guarantee the manufacturing quality and fast dynamic response result in a set of challenging problems for robotic control.

Currently, most applications of industrial robots are based on movement among waypoints which results in relative "rugged" performance, especially when it comes to accurate and continuous path tracking. For example, current industrial welding robots are articulated arms with a preprogrammed set of movements based on separate waypoints, such as 'MoveL' command of Universal Robot (UR), which leads to a discontinuous movement as the robot has to stop after each waypoint. Although 'MoveP', a movement type intended for processes, can be employed to achieve a continuous movement, it will lose the real-time input to modify the path during the whole process which means the human-robot collaboration is failed to be provided. This emphasizes the need for advanced control methods which can make the robots more able to mimic the capabilities (e.g. path and velocity "smoothness") of human operators and be open to accept real-time corrections to fulfil critical applications. A Radial Basis Function Neural network (RBFNNs) was introduced for industrial robot manipulators to deal with uncertain dynamical environments [6]. The adaptive parameter estimation and control for nonlinear robotic systems were also developed in [7]. An adaptive control method was developed to improve the tracking performance of 6 DoF industrial robots. Compared with conventional PID control, the proposed control method can achieve a smaller tracking error when external disturbances and parametric uncertainties are taken into consideration [8]. A sliding mode controller is applied as position controller for compliant mechanics to improve the tracking and disturbance response [9]. However, these research studies focused on position control. How to regulate the velocity and perform smooth movement during the operation process still remains to be further investigated. If the robots could present similar smoothness in movements as human limbs, this would provide a direct link from human intelligence to robotics.

In relation to smoothness/stable motion of robots, a fuzzy logic based controller was proposed to reduce motion chattering phenomena on a wheeled mobile robot [10]. Also, time optimal controller that allows the smooth control of rigid robotic manipulators was designed based on high-order kinematic variables [11]. Jerk-limited trajectory planning methods have also been proposed to reduce vibrations of robotic motions [12]–[14]. However, these research results focus on path planning rather than the actual output with smoothness for robotic systems.

Model predictive control (MPC) has received considerable attention in past decades due to its online optimization capability considering state and input constraints [15], [16]. Compared with traditional optimal control, the online optimization feature of MPC can update the optimal control sequence of the system [17]. Therefore, control strategies based on the MPC concept have found wide acceptance in industrial applications

This work was supported by Innovate UK under Grant REINSTATE: Repair, Enhanced Inspection, and Novel Sensing Techniques for increased Availability and reduced Through Life Expense (TS/V005103/1). (Corresponding author: Abdelkhalick Mohammad.)

T. Zeng, A. Mohammad, A. Madrigal and D. Axinte are with the Rolls-Royce UTC in Manufacturing and On-Wing Technology, University of Nottingham, NG8 1BB, UK. (e-mail: Tianyi.Zeng@nottingham.ac.uk; Abd.Mohammad1@nottingham.ac.uk; Andres.Gamos@nottingham.ac.uk; Dragos.Axinte@nottingham.ac.uk)

Max Keedwell is with Rolls-Royce plc., Bristol, BS34 7QE, UK. (e-mail: Max.Keedwell@rolls-royce.com)

and have been widely studied by academia. Particularly, the MPC approaches have been developed for industrial robotics. A remote control scheme based on MPC was proposed for welding [18]. The influence caused by the external disturbance of the system was remained to be further investigated. A control scheme combines MPC and SMC was developed in [19] so that the MPC can be achieved based on a system with reduced uncertainty. Such control scheme has been applied to robotic system [20]. However, although many control methods have been proved that can be used in open architectures [21]–[23], such as servo motors, how to utilise this method to real robot and guarantee the smoothness based on such control scheme is still to be investigated. Most of the industrial robots' controllers including the UR, are closed architecture (i.e., the control designer has no access to the low-level control). Furthermore, existing standards [24] and methods of human-robot collaborative systems are focused on safety concerns, such as obstacle avoidance [25]. To introduce human skills and experience into the robotic system, the collaboration between human and robots should not only remain on the obstacle avoidance, but also be extended to response human input in the real-time with satisfactory control performance. Despite MPC and SMC has been used in industrial system, up to date, there is no industrial robot that able to accept human inputs (e.g., fine adjustment from expert welder) during executing a predefined path with given speed and trajectory. Design robotic systems with human-robot collaboration and capability of mimicking the operation of skilled operators will dramatically reduce the maintenance cost and downtime in the industry as they can provide efficient critical operations (e.g. repair for specific component shapes), reduce scrap rates, increase overhaul profitability, and reduce CO_2 emissions during the whole maintenances process.

To address these gaps stated above, this paper reports on a control algorithm that allows the smooth arbitrary path of multi-DoF robots capable to mimic human movement. We took further this new capability and integrate the robot with human experiences (i.e. a database of human hand movement with an end-effector) so that the trajectories of humans can be replicated by the robot in real-time. This opens the avenue that actually the robot movements can be corrected in real-time when the human/any other sensing device can observe deviations not only in trajectory but also in “smoothness”. The main contributions of this paper can be summarized as follows.

- A human-robot collaborative system is developed with enhanced smoothness and robustness so that the input from the skilled operator can be responded in the real-time during the path tracking process;
- A control scheme based on MPC and the sliding mode compensator is implemented for both position tracking and speed regulation of industrial robots to follow a predefined trajectory while allowing the expert user to deviate from this desired trajectory in the real-time and in a smooth manner;
- The effectiveness of the proposed control scheme is experimentally verified to guarantee the practical value of such collaborative robotic systems with a wide range of applications.

The rest of this paper is organized as follows. The control-oriented model considering the constraints and external disturbances is established in Section II; The control scheme including online optimization based on MPC and disturbance compensator is developed in Section III; Simulation and experimental results are demonstrated in Section IV to verify the efficacy of the control proposed strategy; Finally, this paper is concluded in Section V.

II. CONTROL-ORIENTED MODEL ESTABLISHMENT

A control-oriented model is established for the path tracking control of the industrial robot. Both the external disturbance and physical constraints are considered in this section. The industrial robot is connected to a computer by an Ethernet cable so that the remote operation can be enabled with an advanced control strategy.

A. Notation

TABLE I
NOTATIONS

Variables in actual system	
x	\triangleq x -axis component of the position
y	\triangleq y -axis component of the position
z	\triangleq z -axis component of the position
Variables in nominal system	
\bar{x}	\triangleq x -axis component of the nominal position
\bar{y}	\triangleq y -axis component of the nominal position
\bar{z}	\triangleq z -axis component of the nominal position
Disturbances	
d_x	\triangleq x -axis component of the external disturbance
d_y	\triangleq y -axis component of the external disturbance
d_z	\triangleq z -axis component of the external disturbance
System parameters	
T_s	\triangleq Sampling time
Controller	
u_x	\triangleq control input along x -axis
u_y	\triangleq control input along y -axis
u_z	\triangleq control input along z -axis
\bar{u}_x	\triangleq nominal control input along x -axis
\bar{u}_y	\triangleq nominal control input along y -axis
\bar{u}_z	\triangleq nominal control input along z -axis

B. Dynamic Model

To achieve a high-performance control for the position of the end effector, the kinetics of the UR and its transformation to the end effector are respectively modelled. This is to consider the control signal is actuated to manipulate the UR directly and to take the vibration from the end effector as well as other external disturbances into account.

The velocity along i -axis is the control input defined as u_i with $i = x, y, z$. Considering the vibration of the end effector and other external disturbances, we have the following dynamic model.

$$\begin{aligned}\dot{x} &= u_x + d_x \\ \dot{y} &= u_y + d_y \\ \dot{z} &= u_z + d_z\end{aligned}\quad (1)$$

and its discrete-time model obtained by zero-order holder is

$$\begin{aligned}x_{k+1} &= x_k + T_s u_{k,x} + T_s d_{k,x} \\ y_{k+1} &= y_k + T_s u_{k,y} + T_s d_{k,y} \\ z_{k+1} &= z_k + T_s u_{k,z} + T_s d_{k,z}\end{aligned}\quad (2)$$

where T_s is the sampling time, x_k , y_k , and z_k are the system states at time $t = t_k$, and $u_{k,x}$, $u_{k,y}$, and $u_{k,z}$ are the system inputs at time $t = t_k$.

The nominal model (disturbance-free model) of (1) is

$$\begin{aligned}\dot{\bar{x}} &= \bar{u}_x \\ \dot{\bar{y}} &= \bar{u}_y \\ \dot{\bar{z}} &= \bar{u}_z\end{aligned}\quad (3)$$

The nominal model (disturbance-free model) of (2) is

$$\begin{aligned}\bar{x}_{k+1} &= \bar{x}_k + T_s \bar{u}_{k,x} \\ \bar{y}_{k+1} &= \bar{y}_k + T_s \bar{u}_{k,y} \\ \bar{z}_{k+1} &= \bar{z}_k + T_s \bar{u}_{k,z}\end{aligned}\quad (4)$$

where \bar{x}_k , \bar{y}_k , and \bar{z}_k are the nominal states at time $t = t_k$, and $\bar{u}_{k,x}$, $\bar{u}_{k,y}$, and $\bar{u}_{k,z}$ are the nominal control inputs at time $t = t_k$.

C. Physical Constraints

During the operation, several physical constraints should be considered. The position should be within safe ranges, which leads to the following state constraints

$$x \in \mathbb{X}, \mathbb{X} = \{x \in \mathbb{R} : x_{min} \leq x \leq x_{max}\} \quad (5)$$

$$y \in \mathbb{Y}, \mathbb{Y} = \{y \in \mathbb{R} : y_{min} \leq y \leq y_{max}\} \quad (6)$$

$$z \in \mathbb{Z}, \mathbb{Z} = \{z \in \mathbb{R} : z_{min} \leq z \leq z_{max}\} \quad (7)$$

where x_{min} , x_{max} , y_{min} , y_{max} , z_{min} , and z_{max} denotes the upper and lower boundaries of the position along three axes, which are constants.

Due to the actuation limitation, the velocities which are also the control inputs should be in reasonable range as follows

$$u_x \in \mathbb{U}_x, \mathbb{U}_x = \{u_x \in \mathbb{R} : |u_x| \leq u_{x,max}\} \quad (8)$$

$$u_y \in \mathbb{U}_y, \mathbb{U}_y = \{u_y \in \mathbb{R} : |u_y| \leq u_{y,max}\} \quad (9)$$

$$u_z \in \mathbb{U}_z, \mathbb{U}_z = \{u_z \in \mathbb{R} : |u_z| \leq u_{z,max}\} \quad (10)$$

where $u_{x,max}$, $u_{y,max}$, and $u_{z,max}$ are the maximum velocities that can be provided along three axes, which are constants.

Assumption 1. The external disturbance caused by vibrations, etc along the i -axis is bounded by a constant $\hat{D}_i > 0$ with $i = x, y, z$.

III. MODEL PREDICTION CONTROL WITH DISTURBANCE REJECTION

In this section, a MPC with SM compensator strategy is proposed to track a pre-planned trajectory subject to unknown external disturbances, uncertainties and multiple constraints. The compensator works on actual model providing disturbance rejection so that MPC can work on the nominal model coping with constraints. Due to the disturbance rejection performance of ISM, and tightened constraints, the original constraints are satisfied and the whole system is robust against disturbances.

A. Overall Strategy

The control system diagram is shown in Fig. 1. A pre-planned trajectory is considered as a desired signal fed into the controller, and with the real-time feedback from the Universal Robot, the proposed controller determines the control action to stabilize the system.

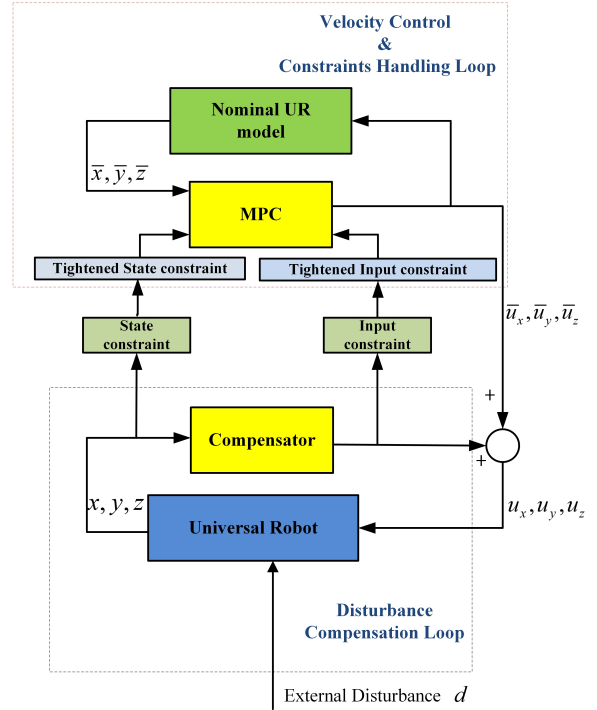


Fig. 1. Control strategy scheme of SM compensator-based MPC with constraints and uncertainties

The control signal of the i -axis contains two components with $i = x, y, z$. One control component, which is the nominal control input, is to stabilize the system and cope with the constraints, and the other one is to cope with the external disturbances which drive the state trajectory away from the desired or pre-planned path. Furthermore, the constraints considered to generate the nominal control input are also tightened from the original constraints to ensure that the original constraints are satisfied in all cases subject to external unknown disturbances.

The control strategy along the i -axis is proposed as

$$u_i = u_{MPC,i} + u_{ISM,i} \quad (11)$$

where $u_{MPC,i}$ is the nominal control input for the velocity control and constraints handling, i.e. $\bar{u}_i = u_{MPC,i}$, and $u_{ISM,i}$ is the compensator for coping with external disturbances, with $i = x, y, z$.

In the following subsections, for simplification purposes, we consider the model of x -axis and design a controller, and then similar results are given for other two axes.

B. MPC Design

The nominal control input $\bar{u}_i = u_{MPC,i}$ is generated based on the nominal model (4). The working principle of MPC is based on a receding horizon strategy where a control sequence is generated by an online optimization, and only the first element of the control sequence is applied to the system.

According to the nominal model (4), we have the following state evolutions along the x -axis

$$\begin{aligned}\bar{x}_{k+1} &= \bar{x}_k + T_s \bar{u}_{k,x} \\ \bar{x}_{k+2} &= \bar{x}_{k+1} + T_s \bar{u}_{k+1,x} \\ &= \bar{x}_k + T_s \bar{u}_{k,x} + T_s \bar{u}_{k+1,x} \\ &\vdots \\ \bar{x}_{k+N} &= \bar{x}_{k+N-1} + T_s \bar{u}_{k+N-1,x}\end{aligned}\quad (12)$$

which gives

$$\begin{bmatrix} \bar{x}_{k+1} \\ \bar{x}_{k+2} \\ \vdots \\ \bar{x}_{k+N} \end{bmatrix} = \begin{bmatrix} 1 \\ 1 \\ \vdots \\ 1 \end{bmatrix} \bar{x}_k + \begin{bmatrix} 1 & 0 & \cdots & \cdots & 0 \\ 1 & 1 & 0 & \cdots & 0 \\ \vdots & \vdots & \ddots & \ddots & 0 \\ 1 & \cdots & \cdots & \cdots & 1 \end{bmatrix} \begin{bmatrix} \bar{u}_{k,x} \\ \bar{u}_{k+1,x} \\ \vdots \\ \bar{u}_{k+N-1,x} \end{bmatrix} T_s \quad (13)$$

where N is the prediction horizon.

Choose the new state vector as

$$X = [\bar{x}_{k+1}, \bar{x}_{k+2}, \dots, \bar{x}_{k+N}]^T \quad (14)$$

and the new input vector as

$$U_x = [\bar{u}_{k,x}, \bar{u}_{k+1,x}, \dots, \bar{u}_{k+N-1,x}]^T \quad (15)$$

The optimization problem over the N -step horizon is

$$\begin{aligned} \mathbb{P}_{N,x} = \arg \min_{[u_{k,x}, \dots, u_{k,x+N-1}]} J_x \\ \text{s.t. } \bar{x}_{k+i} \in \bar{\mathbb{X}} \\ \bar{u}_{k+i,x} \in \bar{\mathbb{U}}_x \end{aligned} \quad (16)$$

where

$$J_x = X^T Q_x X + U_x^T R_x U_x \quad (17)$$

and $\bar{\mathbb{U}}_x$ is the tightened constraint on the input, $\bar{\mathbb{X}}$ is the tightened constraint on the state; Q_x and R_x as constant weight matrices that are positive definite. Consider the nominal model (4), and define the system matrix as $A_x = [1, 1 \cdots 1]^T$ and

$$B_x = T_s \begin{bmatrix} 1 & 0 & \cdots & \cdots & 0 \\ 1 & 1 & 0 & \cdots & 0 \\ \vdots & \vdots & \ddots & \ddots & 0 \\ 1 & \cdots & \cdots & \cdots & 1 \end{bmatrix}, \text{ the cost function (17) can be}$$

rewritten as

$$\bar{J}_x^* = U_x^T H_x U_x + F_x^T U_x \quad (18)$$

where

$$H_x = \frac{1}{2} (B_x^T Q_x B_x + R_x) \quad (19)$$

and

$$F_x^T = \frac{1}{2} x_0 A_x Q_x B_x \quad (20)$$

Therefore, an optimization can be undertaken based on a single input variable U_x , and in MATLAB, it is achieved by 'quadprog' program. Only the first element of the resulted optimal sequence $U_x = [\bar{u}_{k,x}, \bar{u}_{k+1,x}, \dots, \bar{u}_{k+N-1,x}]^T$, which is $\bar{u}_{k,x}$, is applied to the system as the current nominal control input at time $t = t_k$.

Remark 1. (Tightened constraints) Since a compensation control input is introduced to cope with the external disturbances, the input constraints for the MPC subsystem should be tightened to ensure that the total control input does not exceed the limitation. In the sequel, the amplitude of the compensation control input is designed as $K_{ism,i}$ with $i = x, y, z$, therefore, the tightened input constraints $\bar{\mathbb{U}}_i \in \mathbb{U}_i$ are calculated as

$$\bar{\mathbb{U}}_i = \{\bar{u}_i : |\bar{u}_i| \leq u_{i,max} - K_{ism,i}\} \quad (21)$$

with $i = x, y, z$.

In the following subsection, we prove that the nominal state approximates the actual state by applying the compensator, so the tightened constraints on the state are calculated as $\bar{\mathbb{X}} = \mathbb{X}$, $\bar{\mathbb{Y}} = \mathbb{Y}$, and $\bar{\mathbb{Z}} = \mathbb{Z}$.

Following the similar procedure, nominal control inputs along y -axis and z -axis can be achieved.

C. Disturbance Compensator Design

The compensation control input $u_{ISM,x}$ is designed as follows

$$u_{ISM,x} = -K_{ism,x} \text{sign}(s_x) \quad (22)$$

where $K_{ism,x}$ is a positive constant satisfying $K_{ism,x} \geq D_x$ and s_x is sliding variable defined by

$$s_x = L_x [x(t) - x(t_0) - \int_{t_0}^t u_{MPC,x}(\tau) d\tau] \quad (23)$$

with L_x as a positive constant, and the function of $\text{sign}(\Delta)$ is defined by

$$\text{sign}(\Delta) = \begin{cases} \frac{\Delta}{\|\Delta\|} & , \Delta \neq 0 \\ 0 & , \Delta = 0 \end{cases} \quad (24)$$

Theorem 1. By using the compensation control input (22), the unknown external disturbances can be eliminated and the closed-loop dynamics of the actual model approximates the nominal model.

Proof. The proof is divided into two parts. Firstly, we prove that the proposed sliding variable converges to zero and stays at zero afterwards.

Select a Lyapunov candidate as $V = \frac{1}{2} s_x^2$, and its first time derivative is

$$\begin{aligned} \dot{V} &= s_x L_x (\dot{x} - u_{MPC,x}(\tau)) \\ &= s_x L_x (u_{ISM,x} + d_x) \\ &\leq -K_{ism,x} L_x |s_x| + D_x L_x |s_x| \end{aligned} \quad (25)$$

Since $K_{ism,x}$ is set to be $K_{ism,x} > D_x$, we have that $\dot{V} < 0$ holds for any $s_x \neq 0$ and $\dot{V} = 0$ holds only if $s_x = 0$ holds. Therefore, the sliding variable s converges to zero and $s_x = \dot{s}_x = 0$ holds afterwards.

Secondly, we prove that once the sliding mode is maintained, the closed-loop dynamics of the actual model becomes the nominal model.

From $s_x = \dot{s}_x = 0$, we have

$$\dot{s}_x = \dot{x} - u_{MPC,x} = 0 \quad (26)$$

which yields $\dot{x} = u_{MPC,x}$, and since $u_{MPC,x} = \bar{u}_x$ holds, we have $\dot{x} = u_{MPC,x}$. Therefore, the closed-loop dynamics approximates the nominal dynamics. This completes the proof. \square

Similarly, the compensation control inputs along y -axis and z -axis can be obtained as

$$u_{ISM,y} = -K_{ism,y} \text{sign}(s_y) \quad (27)$$

and

$$u_{ISM,z} = -K_{ism,z} \text{sign}(s_z) \quad (28)$$

where $K_{ism,y}$ and $K_{ism,z}$ are positive constants satisfying $K_{ism,y} \geq D_y$ and $K_{ism,z} \geq D_z$, and s_y and s_z are sliding variables defined by

$$s_y = L_y [y(t) - y(t_0) - \int_{t_0}^t u_{MPC,y}(\tau) d\tau] \quad (29)$$

$$s_z = L_z [z(t) - z(t_0) - \int_{t_0}^t u_{MPC,z}(\tau) d\tau] \quad (30)$$

Remark 2. The implementation for practical robotic systems will be influenced by the complexity of the proposed control scheme. SMC is verified to be computational lightweight, but MPC is expected with a higher computational cost. However, with simple constraints and models, the computational burden can be further reduced. A quantified complexity analysis can

be found in [20]. Meanwhile, the prediction horizon should be set with a trade-off between control performance and calculation speed: By choosing a smaller prediction horizon, a faster calculation speed can be achieved but it will lead to a worse control performance. A better control performance can be achieved if a larger prediction horizon is selected as more future information can be introduced during the optimization. However, a slower calculation speed will be obtained. In this study, a 500Hz rate, which is the highest data exchanging rate of Universal Robot, can be guaranteed by the proposed control scheme.

IV. SIMULATION AND EXPERIMENT VALIDATION

In this section, we will testify if the proposed control system can provide a high-enough level of repeatability, accuracy and dynamic response, particularly in highly stressed and difficult to access locations.

A. Test Rig Set-up

The human-robot collaborative is established as shown in Fig. 2. A Universal Robot (UR)-5e with 6 DoF is employed as case studies. The UR-5e is connected by an Ethernet cable with an Intel Xeon 3.5 GHz computer by running a Python program as the developing environment. By using the current set-up, no obvious latency is achieved as the communication frequency between the UR-5e and the computer is 500 Hz which guarantees a fast real-time data exchange. A Xbox One joystick linked to the computer is employed as the real-time human input. The input from the joystick is introduced into the control scheme so that it can be responded during the path tracking process. Multiple kinds of end effectors can be attached to the robot arm so that the proposed control method can be extended to wide inspection and repair tasks even in hazardous environments, such as nuclear and extreme temperatures, where accurate remote control and collaborative robotics based on human experience are needed. The appropriate selection of Q_i and R_i should find a trade-off between the control effort and the performance of the system. The MPC parameters have been selected as $Q_i = \text{diag}(10, 10, 10)$ and $R_i = 0.1$ for each axis, and the rest of controller parameters are shown in Table II. Specifically, $K_{ism,x} \geq D_x$, $K_{ism,y} \geq D_y$ and $K_{ism,z} \geq D_z$ should be satisfied as they are gains of disturbance rejection terms. L_x , L_y and L_z are positive constants that can be tuned carefully to achieve a satisfactory compensation performance.

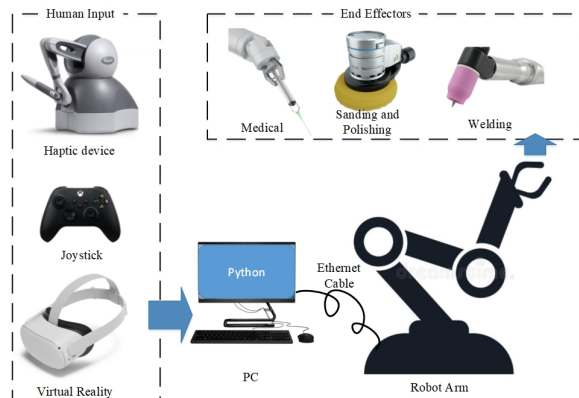


Fig. 2. System overview of the proposed control scheme

TABLE II
CONTROLLER PARAMETERS

Parameter Value	$K_{ism,x}$	$K_{ism,y}$	$K_{ism,z}$	N
	0.6	0.6	0.6	8
Parameter Value	L_x	L_y	L_z	
	0.1	0.1	0.1	

B. Numerical Monte Carlo Analysis

To verify the effectiveness of the proposed control scheme, a simulation of path tracking by using the proposed control scheme and MPC only considering initial error, control input saturation and external disturbance is demonstrated in Fig. 3. Meanwhile, a PID controller, which is widely used in robotics control, is introduced as a comparison.

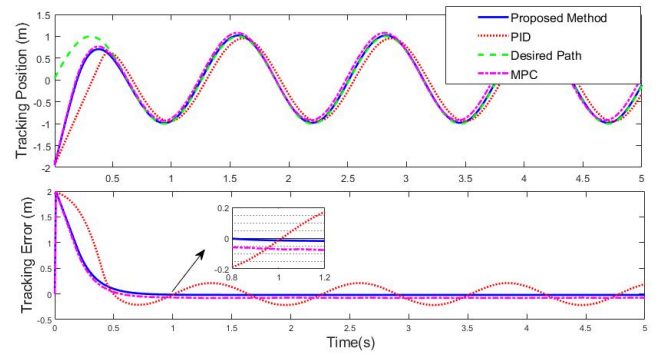


Fig. 3. Tracking performance of the proposed controller in comparison with PID and MPC

It is shown in Fig. 3 that with input constraints and external disturbances, a smaller tracking error can be achieved by the proposed MPC. When the robot is driven to track a path with higher dynamic performance requirement, the superiority of the developed MPC scheme is more obvious as PID will fail to track the desired path when input constraints and external disturbance are taken into consideration. Compared with MPC, the proposed control scheme can further reduce the tracking error as SMC is introduced to tackle uncertainties and external disturbances, and guarantee the robustness of the control system.

To further test the robustness of the proposed control strategy, a numerical Monte Carlo simulation of 200 cases with random initial states and multiple reference signals is demonstrated in Fig. 4. The mean value of the initial position is 0 mm, and the standard deviation of the initial position is 0.4 m, 0.2 m and 0.025 m, respectively for three axes. Meanwhile, a time-varying external disturbance $d = 0.5 \sin(t) + \epsilon$ is introduced in the simulation. Here, $\epsilon \sim N(0, 0.1)$ is a white noise.

Fig. 4 shows that all the axes can converge after 1s and the largest tracking error in the static state can be guaranteed within 3mm for all three axes. Hence, the satisfactory control performance can be achieved with the initial perturbation and the external disturbance which guarantees the robustness and repeatability of the proposed control strategy. Meanwhile, the active input saturations are demonstrated in Fig. 4, which proves the effectiveness of the proposed MPC. We can see that the input constraints are active which bounds the actual control input in the range of $[-0.6, 0.6]$, $[-0.6, 0.6]$ and $[-0.2, 0.2]m/s$ for three axes, respectively. The constraints are set as 60% of UR's speed limitation to make sure the constraints are active. On the other hand, if loose constraints

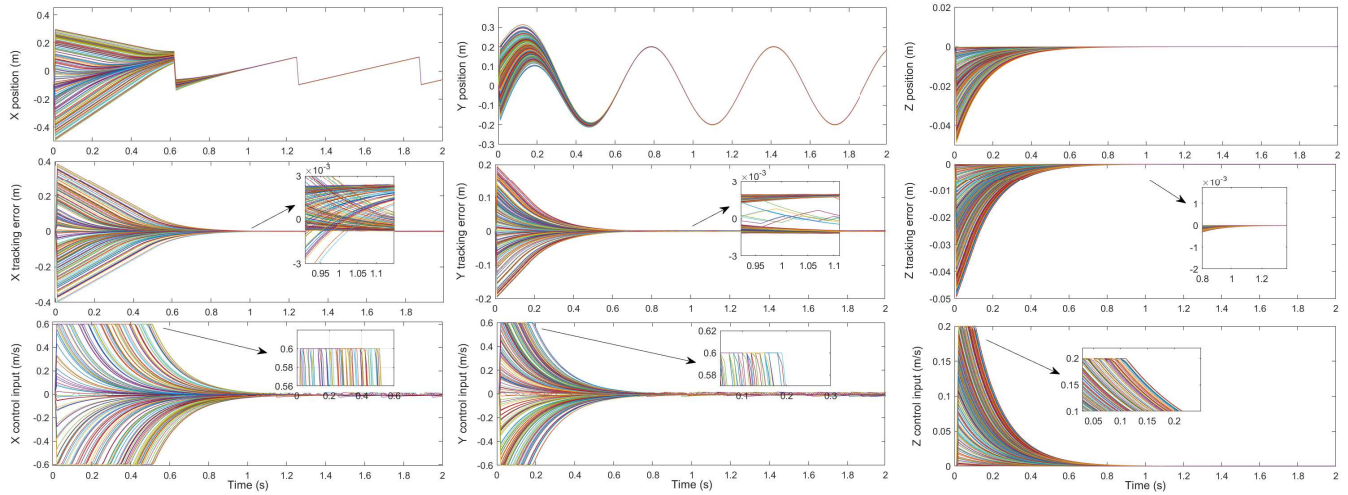


Fig. 4. Tracking performance of Monte Carlo simulation with random initial states, uncertainties and multiple reference signals of 3 axes by using the proposed controller

are set, a better dynamic response and less computational burden can be achieved with a shorter convergence process.

C. Experimental Results

Case 1: Comparison with linear-move strategy

In practical implementation, the signum function can be modified as $\text{sign}(\Delta) = \frac{1}{\|\Delta\| + \mu}$, where μ is an arbitrarily small constant. In this way, the chattering problem can be coped with. Linear-move control command [26], [27] is usually employed to drive the robot move from one waypoint to another in the industrial applications. A comparison of the velocity by using the linear-move control command and the velocity by using the proposed MPC is shown in Fig. 5.

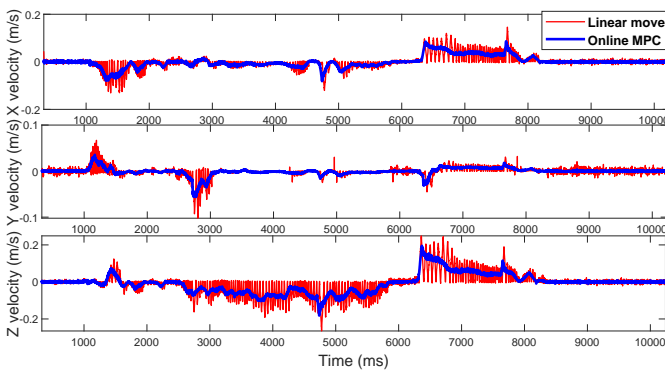


Fig. 5. Velocity comparison between the proposed controller and point-to-point linear-move control strategy

Although the path tracking can be realized by the linear move control command naturally provided by the UR 5e, it should be noticed that the velocity is unsmooth. During the operation process, the quality depends on not only the position control performance but also the velocity. Therefore, the proposed MPC is more suitable than linear move control for the application which needs smooth movement, such as welding and glueing. This is because the proposed method can drive the robot for path tracking by the velocity regulation based on the real-time tracking error. Furthermore, the proposed control scheme is more reliable as the velocity chattering of the linear move is avoided for accurate path tracking.

Case 2: Comparison with open loop velocity control, PID and MPC

Path tracking experimental results are achieved as shown from Fig. 6 to Fig. 7. The desired path is recorded in the free-drive mode of the UR-5e with a 500Hz data exchange rate. To test the robustness of the proposed control scheme, the installation settings of UR is set incorrect on purpose as the uncertainties of the system, and an 1kg extra payload is added during the tracking process as the external disturbance.

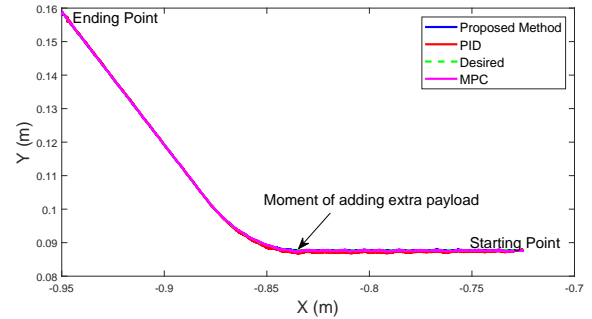


Fig. 6. Tracking trajectory by using the proposed controller in comparison with PID and MPC

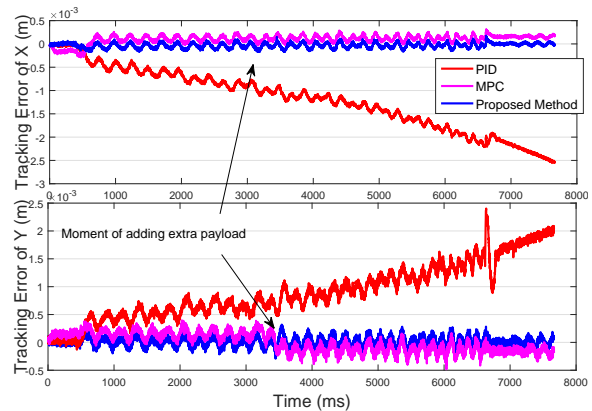


Fig. 7. Tracking error by using the proposed controller in comparison with PID and MPC

As shown above, compared with PID, both MPC and the proposed control scheme can drive the robot for accurate path tracking. However, when a heavier payload (5kg) is employed as the external disturbance, the proposed control scheme can still guarantee the tracking performance as shown in Fig. 8 to Fig. 9.

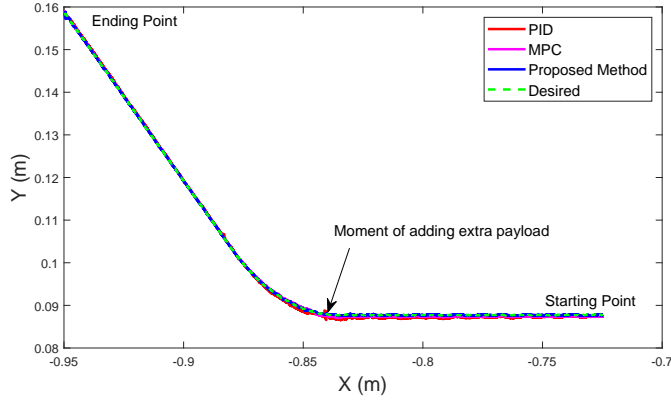


Fig. 8. Tracking trajectory by using the proposed controller in comparison with PID and MPC with larger disturbance

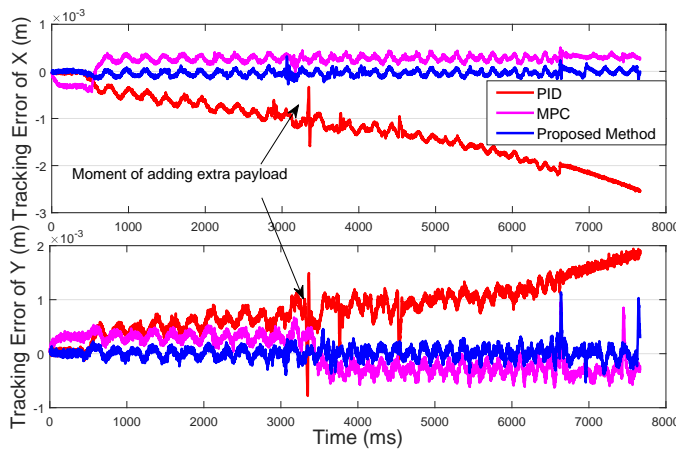


Fig. 9. Tracking error by using the proposed controller in comparison with PID and MPC with larger disturbance

Although PID, MPC and the proposed method can guarantee a smooth path motion compared with linear-move control command, the proposed control scheme can guarantee the accuracy of the path tracking with robustness against uncertainties and disturbances. This is because the tracking error is employed as the input of the proposed controller and a disturbance compensator is introduced in the proposed control scheme so that the robot can be driven accordingly. The robustness provided by the proposed control scheme is desirable for industrial robots application as the control architecture is closed compared to simulation and lab environment (e.g., servo motors) where the controller is open architecture.

Case 3: Path tracking with real-time human input

To modify the recorded path in real-time during a process (e.g. welding) that require high smoothness in path/velocity, a joystick that is linked with the host PC is introduced in the control scheme. The tracking performance of three axes is shown from Fig. 10 to Fig. 11.

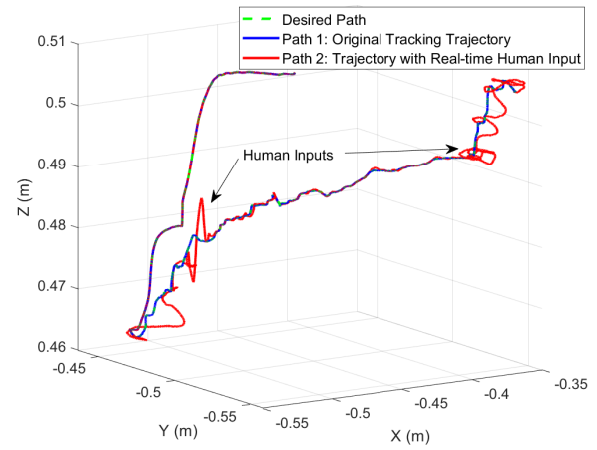


Fig. 10. 3D tracking trajectory with real-time human input by a joystick

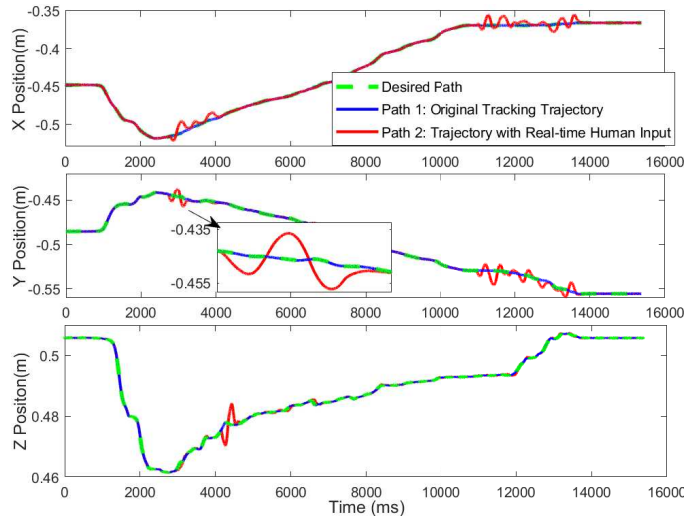


Fig. 11. Tracking performance of 3 axes with joystick real-time input

As shown above, the real-time human intervention can be achieved with a fast dynamic response which guarantees the collaboration between the operator and the robotic system. The maximum distance which can be modified corresponding to the original path is set as 10 mm in this study and it can be tuned according to different scenarios. Meanwhile, it worth to be noticed that the human input will not cause the jerk movement. Therefore, the smoothness can be guaranteed by the proposed human-robot collaborative control system.

Case 4: TIG welding test

To further evaluate the practical effectiveness of the proposed control scheme, a group of TIG welding tests on curved path is presented. The welding torch is attached to UR 5e as shown in Fig. 12. The welding results are shown in Fig. 13.

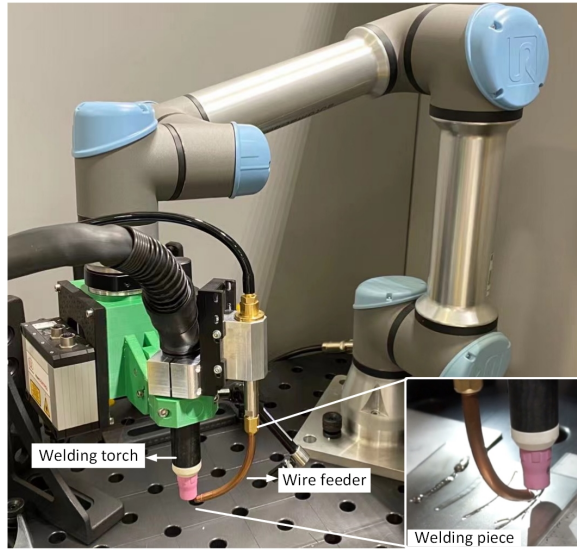


Fig. 12. UR 5e with TIG welding torch

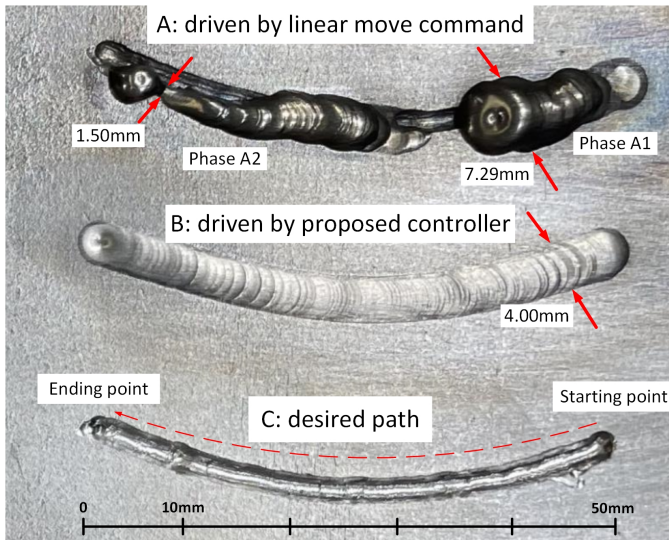


Fig. 13. TIG welding results comparison: (A) welding based on linear move control; (B) welding based on the proposed control scheme; (C) desired path created for case A and B

In Case A, the linear move control based on 10 way-points is employed. The speed vector is set as 1 mm/s during Phase a1 which is the desire speed according to experienced welder, however, the speed is too low which leads too much wire fed in the weld pool. The widest part is 7.29mm as shown in the result. The welding result in Phase a2 is achieved with a higher speed but the speed is not constant which makes the welding lack of quality. The narrowest part can be only 1.50mm. This is because linear move command focus on position control and the speed cannot be constant among waypoints. Note that the speed can be continuous by using 'Move Process' strategy, but it will lose the real-time human input during the whole process. Case B is achieved by using the proposed control scheme with 1mm/s as the desired speed. The smooth movement and stable speed regulation provided by the proposed method guarantees the quality of the TIG welding with a 4.00mm fixed width welding result.

Based on the same desired path shown in Fig. 13 (C), TIG welding based on the proposed control scheme with real-time

human input via a joystick is shown in Fig. 14. We try to add real-time human inputs to weld the Branch 1 and 2 shown in Fig. 14(a) based on the live via a welding camera shown in Fig. 14 (c) to (f).

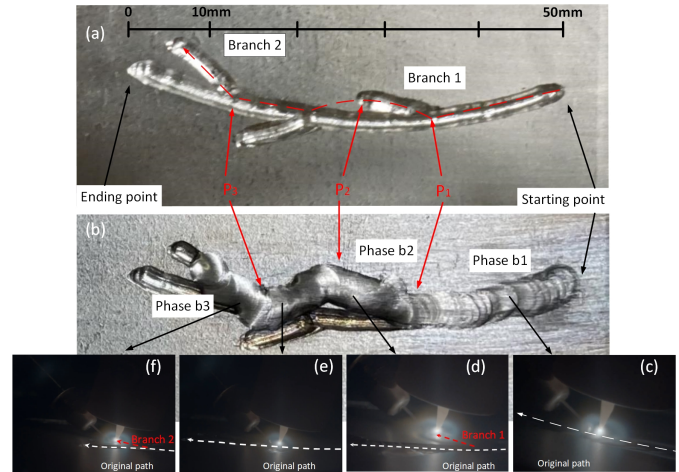


Fig. 14. TIG welding: (a) welding follow the original path; (b) welding with real-time human inputs

In this case, the robot follows the original curved path during Phase b1 and human inputs are added at point P_1 in Phase b2 to follow Branch 1. After welding Branch 1, there is no human input from point P_2 and the robot is back to follow the original path. During Phase b3, human inputs are added again at point P_3 to follow Branch 2. It can be seen in Fig. 14(c) that both the positions and rotations of the welding torch have been changed according to the human input during the welding so that the relative position between the welding torch and the wire feed can be maintained to guarantee the welding quality. Therefore, the experience of the welder can be introduced in the real-time which is critical for the welding in confined spaces that human cannot reach.

V. CONCLUSION

A control strategy based on MPC and sliding mode compensator was designed for the path tracking control of industrial robot. The developed robotic system can be remotely driven by the proposed controller for accurate path tracking control with real-time human modification on the outputted tracking performance. The path tracking with smoothness was empowered by the proposed MPC and the sliding mode disturbance rejection term was designed to compensate the external disturbance so that the control performance of the robotic system can be further improved. Meanwhile, fast dynamic response to the real-time human input can be guaranteed by the proposed control scheme to meet the unique requirement of human-robot collaborative industrial manufacturing and inspection. Simulation and experimental results were demonstrated to verify the effectiveness of the proposed control strategy.

REFERENCES

- [1] M. Ratiu and M. A. Prichici, "Industrial robot trajectory optimization-a review," in *MATEC web of conferences*, vol. 126, p. 02005. EDP Sciences, 2017.
- [2] K. Guo, Y. Zhang, and J. Sun, "Towards stable milling: Principle and application of active contact robotic milling," *International Journal of Machine Tools and Manufacture*, vol. 182, p. 103952, 2022.
- [3] C. B. Smith, "Robotic friction stir welding using a standard industrial robot," *Kei Kinzoku Yosetsu (Journal of Light Metal Welding and Construction)*, vol. 42, no. 3, pp. 40–41, 2004.

[4] J. N. Pires, A. Loureiro, and G. Bölmsjö, *Welding robots: technology, system issues and application*. Springer Science & Business Media, 2006.

[5] Q. Chu, W. Li, D. Wu, X. Liu, S. Hao, Y. Zou, X. Yang, and A. Vairis, "In-depth understanding of material flow behavior and refinement mechanism during bobbin tool friction stir welding," *International Journal of Machine Tools and Manufacture*, vol. 171, p. 103816, 2021.

[6] V. T. Yen, W. Y. Nan, and P. Van Cuong, "Robust adaptive sliding mode neural networks control for industrial robot manipulators," *International Journal of Control, Automation and Systems*, vol. 17, no. 3, pp. 783–792, 2019.

[7] J. Na, M. N. Mahyuddin, G. Herrmann, X. Ren, and P. Barber, "Robust adaptive finite-time parameter estimation and control for robotic systems," *International Journal of Robust and Nonlinear Control*, vol. 25, no. 16, pp. 3045–3071, 2015.

[8] X. Yin and L. Pan, "Enhancing trajectory tracking accuracy for industrial robot with robust adaptive control," *Robotics and Computer-Integrated Manufacturing*, vol. 51, pp. 97–102, 2018.

[9] M. Neubauer, F. Brenner, C. Hinze, and A. Verl, "Cascaded sliding mode position control (smc-pi) for an improved dynamic behavior of elastic feed drives," *International Journal of Machine Tools and Manufacture*, vol. 169, p. 103796, 2021.

[10] Z. Jia, Y. Song, and W. Cai, "Bio-inspired approach for smooth motion control of wheeled mobile robots," *Cognitive Computation*, vol. 5, no. 2, pp. 252–263, 2013.

[11] Y.-S. Lu and Y.-Y. Lin, "Smooth motion control of rigid robotic manipulators with constraints on high-order kinematic variables," *Mechatronics*, vol. 49, pp. 11–25, 2018.

[12] R. Bearee and A. Olabi, "Dissociated jerk-limited trajectory applied to time-varying vibration reduction," *Robotics and Computer-Integrated Manufacturing*, vol. 29, no. 2, pp. 444–453, 2013.

[13] R. Béarée, "New damped-jerk trajectory for vibration reduction," *Control Engineering Practice*, vol. 28, pp. 112–120, 2014.

[14] W. Gao, Q. Tang, J. Yao, and Y. Yang, "Automatic motion planning for complex welding problems by considering angular redundancy," *Robotics and Computer-Integrated Manufacturing*, vol. 62, p. 101862, 2020.

[15] C. E. Garcia, D. M. Prett, and M. Morari, "Model predictive control: Theory and practice—a survey," *Automatica*, vol. 25, no. 3, pp. 335–348, 1989.

[16] S. Zhan, J. Na, G. Li, and B. Wang, "Adaptive model predictive control of wave energy converters," *IEEE Transactions on Sustainable Energy*, vol. 11, no. 1, pp. 229–238, 2018.

[17] Y. Zhang, S. Zhan, and G. Li, "Model predictive control of wave energy converters with prediction error tolerance," *IFAC-PapersOnLine*, vol. 53, no. 2, pp. 12 289–12 294, 2020.

[18] Y. Liu and Y. Zhang, "Toward welding robot with human knowledge: A remotely-controlled approach," *IEEE Transactions on Automation Science and Engineering*, vol. 12, no. 2, pp. 769–774, 2014.

[19] M. Rubagotti, D. M. Raimondo, A. Ferrara, and L. Magni, "Robust model predictive control with integral sliding mode in continuous-time sampled-data nonlinear systems," *IEEE Transactions on Automatic Control*, vol. 56, no. 3, pp. 556–570, 2011.

[20] G. P. Incremona, A. Ferrara, and L. Magni, "Mpc for robot manipulators with integral sliding modes generation," *IEEE/ASME Transactions on Mechatronics*, vol. 22, no. 3, pp. 1299–1307, 2017.

[21] A. E. K. Mohammad, N. Uchiyama, and S. Sano, "Reduction of electrical energy consumed by feed-drive systems using sliding-mode control with a nonlinear sliding surface," *IEEE Transactions on Industrial Electronics*, vol. 61, no. 6, pp. 2875–2882, 2014.

[22] T. Zeng, X. Ren, and Y. Zhang, "Fixed-time sliding mode control and high-gain nonlinearity compensation for dual-motor driving system," *IEEE Transactions on Industrial Informatics*, vol. 16, no. 6, pp. 4090–4098, 2019.

[23] N. Uchiyama, Y. Ogawa, A. E. K. Mohammad, and S. Sano, "Energy saving in five-axis machine tools using synchronous and contouring control and verification by machining experiment," *IEEE Transactions on Industrial Electronics*, vol. 62, no. 9, pp. 5608–5618, 2015.

[24] B. Matthias and T. Reisinger, "Example application of iso/ts 15066 to a collaborative assembly scenario," in *Proceedings of ISR 2016: 47st International Symposium on Robotics*, pp. 1–5. VDE, 2016.

[25] M. Rubagotti, T. Taunyazov, B. Omarali, and A. Shintemirov, "Semi-autonomous robot teleoperation with obstacle avoidance via model predictive control," *IEEE Robotics and Automation Letters*, vol. 4, no. 3, pp. 2746–2753, 2019.

[26] K. Miatliuk, A. Wolniakowski, M. Diaz, M. A. Ferrer, and J. J. Quintana, "Universal robot employment to mimic human writing," in *2019 20th International Carpathian Control Conference (ICCC)*, pp. 1–5. IEEE, 2019.

[27] S. Ponsà Cobas, "Strategies for remote control and teleoperation of a ur robot," Master's thesis, Universitat Politècnica de Catalunya, 2020.



Tianyi Zeng received his B.Eng degree in control science and engineering from Harbin Institute of Technology, Harbin, China, in 2015, and the Ph.D. degree in control science and engineering from Beijing Institute of Technology, Beijing, China, in 2020.

He is currently a research fellow at the Rolls-Royce University Technology Centre (UTC), University of Nottingham, UK. His research interest includes nonlinear system control, plant/controller co-design, and robotic control.



Abdelkhalick Mohammad received the B.Sc. degree in mechatronics engineering from Assiut University, Assiut, Egypt, in 2006, and the M.Eng. and Ph.D. degrees from Toyohashi University of Technology, Toyohashi, Japan, in 2010 and 2013, respectively, both in robotics and mechatronics.

He is currently an Assistant Professor of mechatronics with the Department of Mechanical, Materials and Manufacturing Engineering, University of Nottingham, U.K. His research interests include mechatronics system design, robotics, machine tool control, and control theory.



Andres Gameros Madrigal received the MSc and PhD in manufacturing and mechatronic engineering from the Monterrey Institute of Technology and Higher Education, Mexico in 2012 and 2016 respectively. From there he has been working as a Research Fellow at the Rolls-Royce UTC in manufacturing and On-Wing technology at the University of Nottingham.

He is currently an Assistant Professor in Intelligent Tooling and Specialist Machines at the University of Nottingham. His research interest includes mechanical design, structural analysis, robotics for inspection/repair and design of high precision mechatronic systems for production.



Dragos Axinte is Professor of Manufacturing Engineering in the Faculty of Engineering, University of Nottingham. He is Fellow of the International Academy of Production Engineering (FCIRP). Since 2009 he is the Director of the Rolls-Royce UTC in Manufacturing and On-Wing Technology. His relevant research expertise includes design and development of machine tools and specialist robotic solutions for in-situ repair and maintenance.

He is also Editor-in-Chief of the International Journal of Machine Tools and Manufacture.



Max Keedwell joined Rolls-Royce in 2011 on the Higher Apprenticeship Scheme. Set up the Eurofighter EJ200 engine overhaul facility in RR Filton and was subsequently responsible for engine overhaul and lineside repairs as a Manufacturing Engineer. His current role as Capability Acquisition has included the development of welding processes for high value components and the industrialisation of low-cost robotics into the MRO shops.